Supramolecular Structures and Tautomerism of Carboxylate Salts of Adenine and Pharmaceutically Relevant N^6-substituted Adenine

*Charlene McHugh and Andrea Erxleben**

School of Chemistry, National University of Ireland, Galway, Ireland

ABSTRACT

Co-crystal and salt formation of the kinetin analogue N^6-benzyladenine with the pharmaceutically acceptable co-crystal and salt formers maleic acid, oxalic acid, glutaric acid, succinic acid, benzoic acid and fumaric acid has been studied by solid-state and solvent-drop grinding in combination with X-ray powder diffraction. In all cases salt or co-crystal formation was observed. Single crystals of $(bzadeH^+)(mal^-)$ (**1**) and $(bzadeH^+)_2(ox^{2-})$ (**2**) were obtained by solution crystallization and the X-ray structures are reported along with that of $(adeH^+)_2(mal^-)_2 \cdot ade \cdot 2H_2O$ (**3**) ($bzadeH^+$ = N^6-benzyladeninium, $adeH^+$ = adeninium, ade = adenine, mal^- = hydrogen maleate, ox^{2-} = oxalate). The hydrogen-bonding motifs in **1** - **3** are discussed. The salts contain a robust $bzadeH^+$-carboxylate or ade-carboxylate $R_2^2(9)$ heterosynthon involving the protonated Hoogsteen sites (N6-H, N7-H) of $bzadeH^+$ and ade. Molecular recognition between the protonated Hoogsteen site and the carboxylate group stabilizes the unusual 7H,9H tautomer of $bzadeH^+$ in **2** and the non-canonical 7H-adenine tautomer in **3**.

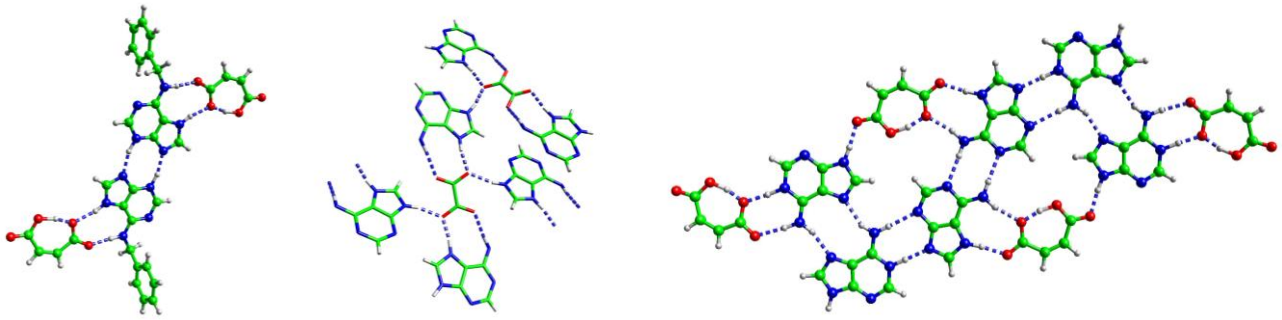

1 **2** **3**

* To whom correspondence should be addressed.

Email: andrea.erxleben@nuigalway.ie. Phone: +353 91 492483. Fax: +353 91 525700

Supramolecular Structures and Tautomerism of Carboxylate Salts of Adenine and Pharmaceutically Relevant N^6-substituted Adenine

*Charlene McHugh and Andrea Erxleben**

School of Chemistry, National University of Ireland, Galway, Ireland.

ABSTRACT

Co-crystal and salt formation of the kinetin analogue N^6-benzyladenine with the pharmaceutically acceptable co-crystal and salt formers maleic acid, oxalic acid, glutaric acid, succinic acid, benzoic acid and fumaric acid has been studied by solid-state and solvent-drop grinding in combination with X-ray powder diffraction. In all cases salt or co-crystal formation was observed. Single crystals of $(bzadeH^+)(mal^-)$ (**1**) and $(bzadeH^+)_2(ox^{2-})$ (**2**) were obtained by solution crystallization and the X-ray structures are reported along with that of $(adeH^+)_2(mal^-)_2 \cdot ade \cdot 2H_2O$ (**3**) ($bzadeH^+$ = N^6-benzyladeninium, $adeH^+$ = adeninium, ade = adenine, mal^- = hydrogen maleate, ox^{2-} = oxalate). The hydrogen-bonding motifs in **1** - **3** are discussed. The salts contain a robust $bzadeH^+$-carboxylate or ade-carboxylate $R_2^2(9)$ heterosynthon involving the protonated Hoogsteen sites (N6-H, N7-H) of $bzadeH^+$ and ade. Molecular recognition between the protonated Hoogsteen site and the carboxylate group stabilizes the unusual 7H,9H tautomer of $bzadeH^+$ in **2** and the non-canonical 7H-adenine tautomer in **3**.

1. INTRODUCTION

N^6-substituted derivatives of the nucleobase adenine exhibit diverse biological activities. They function as plant growth stimulants and have antiallergenic, antibacterial, antiviral and antifungal properties.[1-3] N^6-furfurylaminopurine (kinetin) is a representative of naturally occurring adenine-type cytokinins, a class of plant growth factors that can also act as inhibitors of certain human protein kinases.[4,5] Some kinetin analogues such as olomoucine[6,7] and roscovitine[8] selectively inhibit cyclin-dependent kinases, which play an essential role in the regulation of the cell division cycle,[6,9] and therefore are potent anticancer agents. Roscovitine, for example, has entered clinical trials for the treatment of non-small cell lung cancer and leukemia.

Furthermore, nucleobases have recently been recognized as versatile and flexible supramolecular building blocks.[10] Their propensity to self-assemble *via* hydrogen bonding interactions or metal coordination into larger aggregates has led to a plethora of supramolecular structures, often with intriguing architectures. More recently, more and more structures are emerging where a nucleobase interacts with a complementary small organic molecule to give a hydrogen-bonded network.[10-12] Adenine and its derivatives possess both hydrogen bond acceptor and donor functionalities as well as protonatable nitrogens. Furthermore, adenine can exist in different tautomeric forms with the most stable one being the 9H-amino tautomer (Figure 1).[13-15] Protonation of the 9H-tautomer usually takes place at the N1 nitrogen.[11,16-20] By contrast, while N^6-benzyladenine[21] and kinetin[22] crystallize in the expected 9H-tautomeric form, the N3-protonated 7H-tautomer (Figure 1) was observed in the crystal structures of their bromide, chloride and dihydrogenphosphate salts.[23-26] In recent years the influence of hydrogen bonding interactions and molecular recognition on tautomeric and protonation equilibria has received growing interest and a few examples have been reported in the literature, where a non-canonical nucleobase tautomer is stabilized by a properly positioned H bond acceptor.[27-29]

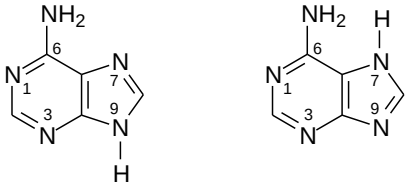

Figure 1. 9H and 7H tautomer of adenine.

Salt and co-crystal formation are popular approaches to optimize the physicochemical properties of a pharmaceutically relevant solid without modifying the molecule itself.[30-32] It is well-established that the solid-state properties of a pharmaceutical solid have a significant impact on drug performance. In many cases, solubility is a key issue. High yields, product purity and reproducibility make salt formation a particularly attractive strategy to address poor solubility.

All of the above prompted us to explore hydrogen bonding patterns in supramolecular structures derived from N^6-benzyladenine as model for pharmaceutically relevant N^6-substituted adenine derivatives and carboxylic acids that are pharmaceutically acceptable salt or co-crystal formers. Here we report the X-ray structures of two N^6-benzyladeninium carboxylates, hydrogen maleate and oxalate, featuring different H bonding networks and different tautomers of the N^6-benzyladeninium cation. To study the influence of the benzyl substituent, co-crystallization experiments have also been carried out with adenine leading to crystals containing both adenine and adeninium cations, with the latter ones in their expected 1H,9H tautomeric form, while the former one exists as 7H-tautomer. Furthermore, we show that the supramolecular networks of benzyladeninium cations and carboxylate anions can be synthesized by solid-state and liquid-assisted grinding. The preparation of salts and co-crystals by solid-state grinding, *i.e.* by grinding together the two solid components with a mortar and pestle or in a mixer mill, is an attractive alternative method to solution crystallization.[33-39] In liquid-assisted grinding, a few drops of solvent are added to the dry mixture to catalyze or mediate co-crystal or salt formation.[40-42] Besides its 'green' nature in that there is no waste of crystallization solvent, solid-state grinding allows for nearly quantitative yields with a common particle size while solubility problems are avoided.

2. MATERIALS AND METHODS

N^6-Benzyladenine and adenine were purchased from Sigma Aldrich. Solvents were of analytical or spectroscopic grade, purchased from commercial sources and used without further purification.

FT-IR spectra were recorded on a PerkinElmer FT-IR spectrometer fitted with a DATR 1 bounce Diamond/ZnSe Universal ATR sampling accessory. Elemental analyses (carbon, hydrogen and nitrogen) were performed with a PerkinElmer 2400 Series II analyser.

Solid-State and Solvent-Drop Grinding. Solid-state and solvent-drop grinding experiments were carried out as follows: N^6-benzyladenine and the respective carboxylic acid (750 mg in total, 1:1, 1:2 or 2:1 molar ratio) were combined with or without the addition of a few drops of methanol, ethanol, acetonitrile or water or one drop of dimethylformamide. The mixtures were ground for 30 minutes in an oscillatory ball mill (Mixer Mill MM400, Retsch GmbH & Co., Germany) at 25 Hz using a 25 cm^3 stainless steel grinding jar and one 12 mm stainless steel ball. Any small amount of solvent present was allowed to evaporate and the resulting material was characterized by X-ray powder diffraction. Solvents, molar ratios and products identified by XRPD are summarized in Table 1.

Preparation of Single Crystals of 1 – 3. Crystallization of 1. 100 mg (0.444 mmol) N^6-benzyladenine and 52 mg (0.448 mmol) maleic acid were dissolved in 10 cm^3 methanol and transferred into a vial with dimensions of 7.5 cm (height) x 2.5 cm (diameter) to allow for slow evaporation of the solvent at room temperature. Colourless, needle-shaped crystals appeared after a few days.

Crystallization of 2. 100 mg (0.444 mmol) N^6-benzyladenine and 56 mg (0.444 mmol) oxalic acid dihydrate were dissolved in 8 cm^3 methanol. The solution was kept in an open beaker (height 7.5 cm x diameter 2.5 cm) at room temperature. Colourless plates crystallized within a week.

Crystallization of 3. 100 mg (0.740 mmol) adenine and 86 mg (0.741 mmol) maleic acid in 15 cm^3 methanol were gently heated (40 °C) until dissolved. Slow evaporation of the solvent at room temperature (open beaker, 7.5 cm (height) x 2.5 cm (diameter)) gave colourless needles within a week.

X-ray Powder Diffraction. X-ray powder patterns of samples obtained by solvent-grinding and crystallization from solution were recorded on an Inel Equinox 3000 powder diffractometer between 5

and 90 ° (2θ) using Cu K_α radiation (λ = 1.54178 Å, 35 kV, 25 mA). Theoretical powder patterns for **1-3** were calculated using the Oscail software package.[43]

Table 1. Solid-State and Solvent-Drop Grinding Experiments

Mixture	Molar Ratio	Solvent	Product
N^6-benzyladenine / maleic acid	1:1	-	**1**
N^6-benzyladenine / maleic acid	1:1	water	**1**
N^6-benzyladenine / maleic acid	1:1	methanol	**1**
N^6-benzyladenine / maleic acid	1:1	ethanol	**1**
N^6-benzyladenine / maleic acid	1:1	dimethylformamide	**1**
N^6-benzyladenine / maleic acid	1:2	methanol	**1**
N^6-benzyladenine / maleic acid	2:1	methanol	**1**
N^6-benzyladenine / oxalic acid	1:1	-	-
N^6-benzyladenine / oxalic acid	1:1	water	**IV** [a]
N^6-benzyladenine / oxalic acid	1:1	methanol	**III** [a]
N^6-benzyladenine / oxalic acid	1:1	acetonitrile	**2**
N^6-benzyladenine / oxalic acid	1:1	dimethylformamide	**2**
N^6-benzyladenine / oxalic acid	2:1	-	**2**
N^6-benzyladenine / oxalic acid	2:1	methanol	**2**
N^6-benzyladenine / oxalic acid	2:1	water	**2**
N^6-benzyladenine / oxalic acid	2:1	acetonitrile	**2**
N^6-benzyladenine / oxalic acid	2:1	dimethylformamide	**2**
N^6-benzyladenine / glutaric acid	1:1	methanol	[b]
N^6-benzyladenine / succinic acid	1:1	methanol	[b]
N^6-benzyladenine / benzoic acid	1:1	methanol	[b]
N^6-benzyladenine / fumaric acid	1:1	methanol	[b]

[a] see text. [b] The XRPD pattern is different from that of a physical mixture of the starting compounds, but the product could not be further characterized.

Crystal Structure Determination and Refinement. Crystal data for **1 - 3** were collected at room temperature on an OxfordDiffraction Xcalibur CCD diffractometer using graphite-monochromated Mo-K_α radiation (λ= 0.71069 Å).[44] The structures were solved by direct methods and subsequent Fourier syntheses and refined by full-matrix least squares on F^2 using SHELXS-97,[45] SHELXL-97[45] and Oscail.[43] The scattering factors were those given in the SHELXL program. Hydrogen atoms were located in the difference Fourier maps and refined isotropically. Graphics were produced with ORTEX.[43] Crystallographic data and details of refinement are reported in Table 2.

Table 2. Crystallographic Data for Compounds 1 - 3

	1	**2**	**3**
Formula	$C_{16}H_{15}N_5O_4$	$C_{13}H_{12}N_5O_2$	$C_{23}H_{27}N_{15}O_{10}$
M_r	341.33	540.56	673.60
Crystal colour and habit	colourless needle	colourless plate	colourless needle
Crystal size (mm)	0.30 x 0.10 x 0.10	0.30 x 0.30 x 0.15	0.40 x 0.20 x 0.20
Crystal system	monoclinic	monoclinic	monoclinic
Space group	$P2_1/n$	$P2_1/c$	$P2_1/c$
Unit cell dimensions			
a [Å]	9.022(1)	8.4126(4)	13.8273(9)
b [Å]	5.1904(5)	11.7538(4)	16.7538(9)
c [Å]	33.712(3)	13.5103(6)	13.0832(9)
β [°]	95.61(1)	103.951(5)	100.822(6)
V [Å^3]	1571.0(3)	1296.5(1)	2976.9(3)
Z	4	4	4
D_{calc} (g cm^{-3})	1.439	1.385	1.503
μ(Mo Kα) (cm^{-1})	1.07	0.99	1.21
F(000)	712	564	1400
2θ range (°)	7.2 - 50.0	6.1 - 52.8	6.3 - 51.4
No. measd. reflections	5369	5142	11679
No. unique reflections (R_{int})	2772 (4.1 %)	2643 (2.3 %)	5631 (4.9%)
No. observed reflections	1718 ($I > 2\sigma(I)$)	2034 ($I > 2\sigma(I)$)	2578 ($I > 2\sigma(I)$)
No. parameters	274	229	541
Final R_1, wR_2	R_1 = 7.4%,	R_1 = 4.1%,	R_1 = 5.4%,
(observed reflections) [a]	wR_2 = 12.9%	wR_2 = 9.7%	wR_2 = 7.9%
Goodness-of-fit	1.142	1.041	0.901
(observed reflections)			

[a] $R_1 = \Sigma|\,|F_o| - |F_c|\,| / \Sigma|F_o|$; $wR_2 = [\Sigma w(F_o^2 - F_c^2)^2 / \Sigma w(F_o^2)^2]^{1/2}$; $w^{-1} = \sigma^2(F_o^2) + (aP)^2$; $P = (F_o^2 + 2F_c^2)/3$.

Supplementary crystallographic data have been deposited with the Cambridge Crystallographic Data Centre, CCDC no. 834877 (**1**), 834878 (**2**) and 834879 (**3**). Copies of the data may be obtained free of charge from The Director, CCDC, 12 Union Road, Cambridge CB2 1EZ, UK (fax:+44-1223-336033; e-mail: deposit@ccdc.cam.ac.uk or www: http://www.ccdc.cam.ac.uk).

3. RESULTS

Solid-State and Liquid-Assisted Grinding of N^6-Benzyladenine – Carboxylic Acid Mixtures. To study the formation of salts or co-crystals of N^6-benzyladenine (bzade) and carboxylic acids by solid-state grinding, 1:1 mixtures of the adenine derivative and a carboxylic acid were ground in a mixer mill and analysed by X-ray powder diffraction (XRPD). Figure 2a shows the XRPD patterns of bzade – maleic acid mixtures after different milling times. Broad and poorly resolved peaks were observed after after 5 minutes of grinding, indicating partial amorphisation. Upon further grinding, the XRPD pattern (designated as pattern **I**) became sharp and clearly differed from that of a physical mixture of bzade and maleic acid (see Figure 2b for individual XRPD patterns of bzade and maleic acid). After 20 minutes the transformation of the XRPD pattern was complete and longer milling times did not result in any further changes. The effect of solvent-assisted grinding was studied by adding a few drops of methanol, ethanol, dimethylformamide or water to the mixture. In each case, a powder pattern identical to **I** was obtained except that the peaks were sharper and better resolved (see Supporting Information, Figure S1). The absence of characteristic peaks from bzade at 18.5, 19.4 and 26.3° (2θ) and from maleic acid at 28.5° (2θ) indicated that the transformation was quantitative. Mixing bzade and maleic acid in a 2:1 or 1:2 ratio gave the same product pattern **I** besides peaks due to excess bzade or maleic acid (Figure 2b).

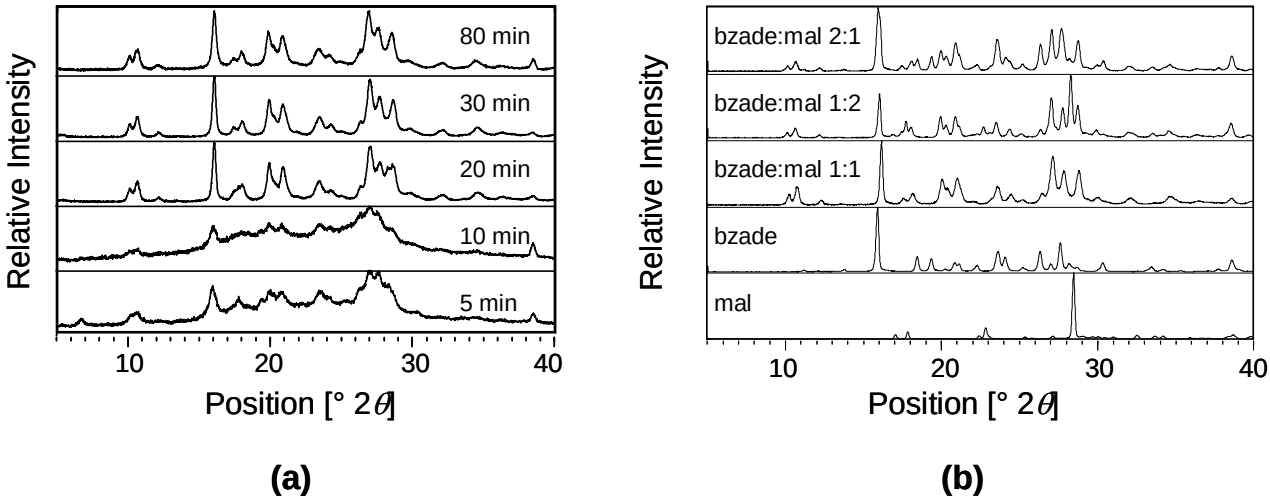

Figure 2. (a) XRPD patterns of a 1:1 mixture of bzade and maleic acid after different milling times. (b) XRPD patterns of bzade, maleic acid (mal) and 1:1, 1:2 and 2:1 mixtures of bzade and maleic acid after 20 min. of solvent-drop (methanol) grinding.

In contrast to maleic acid, milling of oxalic acid with an equimolar amount of bzade in the absence of solvent did not result in any transformation. The XRPD pattern recorded after 20 minutes of dry-grinding was that of a physical mixture of bzade and oxalic acid. However, a new set of XRPD peaks emerged upon milling in the presence of a small amount of acetonitrile or dimethylformamide (Figure 3 and Supporting Information, Figure S2). A similar pattern (designated as pattern **II**) was obtained, when the bzade : acid ratio was 2:1. In contrast to the 1:1 mixture, where no transformation was observed in the absence of a small amount of solvent, dry-grinding of a 2:1 mixture gave a product pattern identical to **II** (Figure 3). Likewise, pattern **II** was observed, when 2:1 mixtures were milled in the presence of a few drops of methanol or water (see Supporting Information, Figure S3). By contrast, the addition of methanol or water to a 1:1 mixture resulted in XRPD patterns that were different from **II** and different from each other (patterns **III** and **IV**, see Supporting Information, Figure S2).

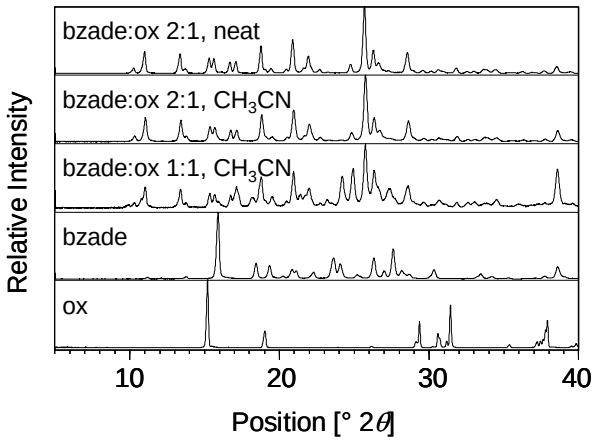

Figure 3. XRPD patterns of bzade, oxalic acid (ox) and 1:1 and 2:1 mixtures of bzade and oxalic acid after 20 minutes of dry- and solvent-drop (CH_3CN) grinding.

Solvent-assisted grinding experiments were also carried out with the following acids; glutaric acid, succinic acid, benzoic acid and fumaric acid. In all cases, changes in the XRPD patterns of 1:1 mixtures suggested salt or co-crystal formation (see Supporting Information, Figure S4).

Solution Crystallization. Slow evaporation of methanol or dimethylformamide solutions of 1:1 mixtures of bzade and glutaric acid, succinic acid, benzoic acid or fumaric acid gave powders or very thin needles unsuitable for single-crystal X-ray analysis. X-ray suitable crystals were obtained with oxalic acid and maleic acid. The salt $(bzadeH^+)(mal^-)$ (mal^- = hydrogen maleate) (**1**) crystallized from methanol, while crystals of composition $(bzadeH^+)_2(ox^{2-})$ (ox^{2-} = oxalate dianion) (**2**) formed upon slow evaporation of a 1:1 mixture of bzade and oxalic acid in methanol or dimethylformamide. It is generally accepted that salts will be obtained, when the difference between the pK_a values of the base and the acid, ΔpK_a, is > 3, while a $\Delta pK_a < 0$ will lead to a co-crystal. For $0 < \Delta pK_a < 3$, co-crystals, salts or mixed ionization complexes can result.[46] The pK_{a1} and pK_{a2} values of oxalic and maleic acid are 1.2 and 4.2[47] and 1.9 and 6.9,[48] respectively. For bzade a pK_a value of 3.9 has been reported[49] so that the difference between the pK_a values of bzade and the first pK_a value of maleic and oxalic acid fall in the overlap range where salt or co-crystal formation is not predictable (ΔpK_a = 2.0 and 2.7, respectively). Single-crystal X-ray analysis of **1** and **2** clearly revealed that proton transfer from the carboxylic acid to bzade

had taken place with maleic acid forming the monoanion and oxalic acid forming the dianion. Considering the second pK_a value of oxalic acid, formation of the salt of the dianion is not necessarily expected, although the ΔpK_a value of -0.3 is close to the overlap region.

To ensure that the single-crystal structures determined for **1** and **2** are representative for the bulk composition of the crystalline materials, theoretical powder patterns were generated form the single crystal data. In both cases, the simulated powder pattern matches with that measured for the isolated crystalline sample (Supporting Information, Figures S5 and S6). Furthermore, the XRPD patterns of the isolated crystals of **1** and **2** were found to be identical to patterns **I** and **II** obtained by dry- and solvent-drop grinding (Supporting Information, Figures S5 and S6), demonstrating that milling and crystallization from solution lead to the same structures. It should be noted that crystallization from methanolic solution gave **2** irrespective of the molar ratio. The compound corresponding to pattern **III** that was observed upon methanol-assisted grinding of 1:1 mixtures of bzade and oxalic acid did not crystallize. Crystallization experiments from aqueous solution to obtain the product giving pattern **IV** were unsuccessful due to the poor solubility of bzade in water.

Crystal Structure of (bzadeH$^+$)(mal$^-$) (1). 1 has a 1:1 stoichiometry and consists of a hydrogen maleate anion and an *N*^{6}-benzyladeninium cation (Figure 4a). Like the cations in *N*^{6}-benzyladeninium bromide[23] and kinetin hydrochloride[24], bzadeH$^+$ exists as H3,H7-tautomer. The hydrogen atoms have been located in the difference Fourier map and refined isotropically. Further evidence for the transfer of one proton from maleic acid to bzade and for the positions of the hydrogens in the heterocycle comes from the C-O bond lengths and from the bond angles of the endocyclic nitrogens. The internal angles at N(7) and N(9) are 106.4(3)° and 102.6(3)° in **1**, compared to 103.9(2)° and 106.4(2)° in 9H-benzadenine.[21] The increase of the C(5)-N(7)-C(8) bond angle by 2.5° and the decrease of the C(4)-N(9)-C(8) bond angle are indicative of the shift of the N(9) hydrogen to N(7).[23,24,50] Likewise, the widening of the C(2)-N(3)-C(4) bond angle from 110.7(2)° in bzade[21] to 116.4(3)° in **1** is consistent with the N(3) nitrogen being protonated. By contrast, the C(2)-N(1)-C(6) bond angle in **1** (119.7(3)°) is

close to that observed in neutral bzade (118.2(2)°),[21] corroborating that N(1) is unprotonated. The structural parameters of the counterion are in line with the formation of the mono anion. For one of the carboxyl groups clearly distinct C-O and C=O bond lengths are observed (1.208(4) Å and 1.297(4) Å), while for the second one, the difference between the two C-O bonds (1.237(4) and 1.267(4) Å) is 0.03 Å. A difference of ≤ 0.03 Å between the C-O bonds is characteristic of a deprotonated carboxylate group, while in a protonated carboxyl group the C-O bonds differ by ≥ 0.08 Å.[46] The carboxyl proton of the hydrogen maleate anion is held in an extremely short intramolecular H bond. The H atom is approximately centred between O(2) and O(4) with O(2)···H, O(4)···H and O(2)···H···O(4) being 1.23(5) Å, 1.28(5) Å and 167(5)°, respectively. A short, symmetrical or approximately symmetrical intramolecular O···H···O hydrogen bond has been found in several crystal structures of hydrogen maleate anions.[51-53]

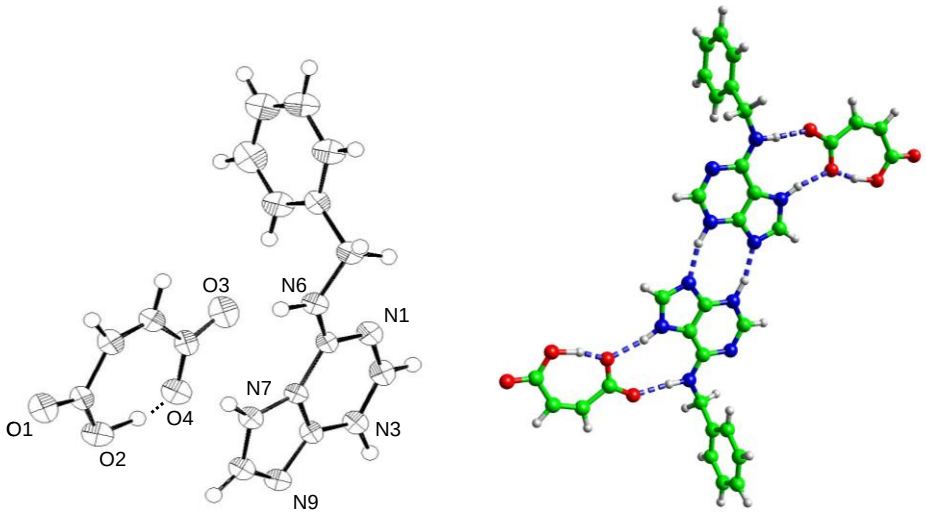

Figure 4. (a) Asymmetric unit of **1**. Thermal ellipsoids are drawn at the 30 % probability level. (b) Hydrogen bonding motif in **1**.

Figure 4b shows the hydrogen bonding motif in **1**. Hydrogen bond distances and angles are listed in Table 3. Centrosymmetric bzadeH$^+$- bzadeH$^+$ dimers with a planar $R_2^2(8)$ motif are formed by pairs of N(3)-H···N(9) hydrogen bonds. The Hoogsteen sites (N(6)-H, N(7)-H) of the bzadeH$^+$···bzadeH$^+$ base pair form hydrogen bonds to the anions with an $R_2^2(9)$ pattern so that overall a mal···bzadeH$^+$···bzade$^+$···mal motif is generated. N(1) is the only nitrogen that is not involved in H bonding. Hydrogen bonding *via* N(1) is prevented by the substituent at the N^6 position which is distal to the imidazole ring. The same effect of the N^6 substituent is observed in the solid-state structures of kinetin,[22] kinetin hydrochloride[24] and dihydrogen phosphate,[25] N^6-benzyladenine[21] and N^6-benzyladenine hydrobromide.[23] In all cases the N^6 substituent adopts a distal conformation and N(1) does not participate in hydrogen bonding. Further extension of the supramolecular structure reveals C-H···O hydrogen bonds between C(2)-H and C(8)-H of the purine and C=O of the hydrogen maleate anion, leading to a $R_2^1(8)$ ring formation.

Table 3. Hydrogen bonding in 1 (Å, °)

D-H···A [a]	d(D-H)	d(H···A)	d(D···A)	∠(DHA)
N(6)-H(6)···O(3)	1.00(3)	1.74(3)	2.733(4)	174(3)
N(7)-H(7)···O(4)	0.97(4)	1.82(4)	2.775(4)	167(3)
N(3)-H(3)···N(9)$^{\#1}$	1.06(4)	1.82(4)	2.842(4)	164(4)
C(2)-H(2)···O(1)$^{\#2}$	0.97(4)	2.27(4)	3.063(5)	138(3)
C(8)-H(8)···O(1)$^{\#3}$	0.96(3)	2.40(3)	3.110(5)	130(3)
O(2)···H(2a)···O(4)	1.23(5)	1.28(5)	2.486(4)	167(5)

[a] symmetry operation: #1: -x,2-y,-z; #2: 1+x,2+y,z; #3: -x-1,-y,-z

Crystal Structure of (bzadeH$^+$)$_2$(ox^{2-}) (2). X-ray analysis of **2** revealed a 2:1 stoichiometry of bzadeH$^+$ cations and oxalate dianions assembled into an infinite 2D H bonded network. Geometric parameters of the hydrogen bonding interactions are presented in Table 4. In contrast to **1**, the bzadeH$^+$

cation in **2** has hydrogens at N(7) and N(9) which have been found in the difference Fourier map. The crystallization of the unusual 7H,9H-tautomer is further corroborated by the bond angles of the endocyclic nitrogens. The C(5)-N(7)-C(8) angle is almost 4° larger than in neutral bzade (107.6(1) *vs.* 103.9(2)° [21]), while the C(4)-N(9)-C(8), C(2)-N(3)-C(4) and C(2)-N(1)-C(6) bond angles (107.9(1), 110.7(1) and 118.6(1)°) are close to those reported for 9H-bzade (106.4(2) for N(9), 110.7(2)° for N(3) and 118.1(2)° for N(1)[21]). As in **1**, the orientation of the phenyl ring is distal to the purine imidazole ring allowing for H bonding to a carboxylate group *via* the Hoogsteen site in a $R_2^2(9)$ pattern. As the oxalate dianion is situated on an inversion centre, this H bonding interaction generates a $bzadeH^+\cdots ox^{2-}\cdots bzadeH^+$ motif (Figure 5a). The dihedral angle between the phenyl ring and the purine plane is 49.23(6)° and is much smaller than in $bzadeH^+Br^-$ (108.4(1)° [23]), neutral bzade (78.5(3)° [21]), and **1** (84.7(2)°) where the phenyl and purine rings are approximately at right angle to each other. The phenyl ring is tilted towards the Hoogsteen site. This forces the oxalate oxygen O(2) out of the adenine ring plane so that in contrast to **1** the $R_2^2(9)$ ring is non-planar (Figure 5b). The distance between O(2) and the centroid of the phenyl ring is 4.49(1) Å.

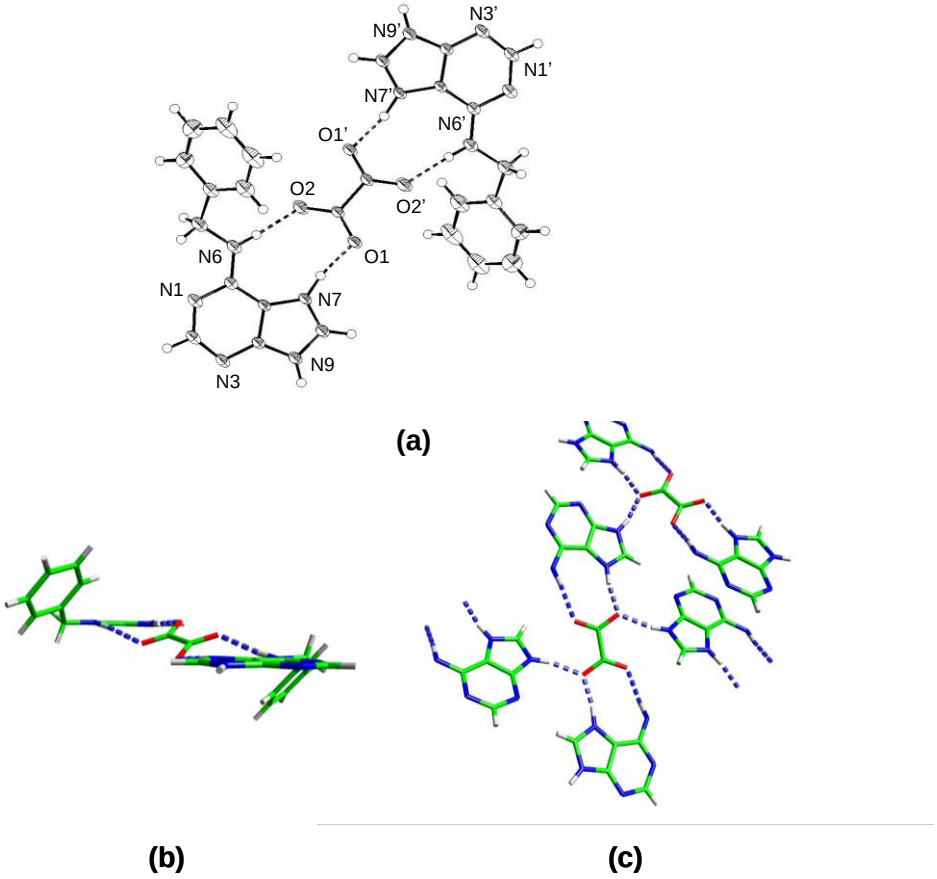

Figure 5. (a) bzadeH^{+}···ox^{2-}···bzadeH^{+} motif in **2.** Thermal ellipsoids are drawn at the 30 % probability level. (b) Side view of the bzadeH^{+}···ox^{2-}···bzadeH^{+} motif**.** (c) Details of H bonding interactions in **2**. The benzyl substituent is omitted for clarity.

Figure 5c shows further details of the hydrogen bonding interactions. H bonds between N(9)-H and carboxylate oxygen link the bzadeH^{+}···ox^{2-}···bzadeH^{+} entities into an infinite 2D network. In addition, C-H···N hydrogen bonding is observed between C(8)-H and N(3) at -x,½+y,½-z. In contrast to the bzadeH^{+}···bzadeH^{+}···mal^{-} motif in **1,** there is no pairing between bzadeH^{+} cations. As in **1**, the N(1) nitrogen does not participate in H bonding.

Table 4. Hydrogen bonding in 2 (Å, °)

D-H···A [a]	d(D-H)	d(H···A)	d(D···A)	∠(DHA)
N(6)-H(6)···O(2)	0.91(2)	1.99(2)	2.89(2)	174(2)
N(7)-H(7)···O(1)	0.98(2)	1.66(2)	2.628(2)	169(2)
N(9)-H(9)···O(1)$^{\#1}$	0.92(2)	1.79(2)	2.685(2)	167(2)
N(9)-H(9)···O(2)$^{\#2}$	0.92(2)	2.37(2)	2.865(2)	114(1)
C(8)-H(8)···N(3)$^{\#3}$	0.97(2)	2.523(2)	3.449(2)	159(1)

[a] symmetry operation: #1: -x,-1/2+y,1/2-z; #2: x,3/2-y,1/2+z; #3: -x,1/2+y,1/2-z

Co-crystallization of Adenine with Oxalic Acid and Maleic Acid. To investigate the influence of the N^6-substituent on the association patterns, co-crystallization experiments were carried out with adenine and oxalic and maleic acid. Slow evaporation of an aqueous solution containing equimolar amounts of adenine and maleic acid gave needle-shaped crystals which were characterized by X-ray analysis as $(adeH^+)_2(mal^-)_2 \cdot ade \cdot 2H_2O$ (**3**) (ade = adenine). The theoretical powder pattern calculated form the crystal data is in good agreement with the powder pattern obtained from the isolated crystalline sample demonstrating that the single-crystal structure represents the composition of the bulk material (see Supporting Information, Figure S7). Unfortunately, all attempts to grow single crystals of an adeninium oxalate salt were unsuccessful. Mixing solutions of adenine and oxalic acid in water, dimethylsulfoxide, dimethylformamide and methanol invariably gave insoluble powders. The XRPD pattern of the powder isolated from a methanolic solution clearly differs from that of a physical mixture of oxalic acid and adenine (data not shown). The IR data also suggest salt formation: The ν(C=O) and $\delta_{sciss}(NH_2)$ vibrations that appear at 1665 and 1671 cm^{-1} in the spectrum of the starting compounds coincide as a broad band at 1684 cm^{-1}. The bands at 1238 and 1437 cm^{-1} that are ascribed to the symmetric stretching modes of C-O, C-C and O-C=O bonds and to the symmetric stretching and bending mode of C-O and O-C=O bonds in free oxalic acid are not observed in the IR spectrum of the

reaction product. Likewise, the C-N and C-C stretching vibrations of free adenine at 1333, 1307 and 1126 cm^{-1} are shifted in the product spectrum. The $\rho(NH_2)$ vibration that appears at 1603 cm^{-1} in the IR spectrum of free adenine is observed at 1592 cm^{-1}. The elemental analysis is consistent with a 1:1 stoichiometry (found C, 37.52; H, 3.11; N, 30.56; calculated for $C_7H_7N_5O_4$: C, 37.34; H, 3.13, N, 31.10%).

Crystal Structure of $(adeH^+)_2(mal^-)_2 \cdot ade \cdot 2H_2O$ (3). The asymmetric unit of **3** consists of two adeninium cations in their 1H,9H-tautomeric forms, two hydrogen maleate anions, one neutral adenine and two water molecules of crystallization. Interestingly, the neutral adenine exists as the minor 7H-tautomer. The presence of the non-canonical tautomer has been unambiguously determined by the location of the H7 proton in the difference Fourier map. Furthermore, the 7H-tautomer of adenine is confirmed by the observed hydrogen-bonding interactions with the hydrogen maleate anion (see below) and by the endocyclic C-N-C bond angles. The C(8)-N(7)-C(5) angle (105.5(3)°) is approximately 2° larger than the C(8)-N(9)-C(4) angle (103.4(3)°). Similar values have been reported for the angles in N^6-benzoyladenine that crystallizes as 7H-tautomer (C(8)-N(7)-C(5) 106.7(3)°; C(8)-N(9)-C(4) 103.2(3)°).[54] The two adeninium cations exhibit the usual features of the 9H-tautomer protonated at N(1). As in **1**, the hydrogen maleate anions feature a strong, extremely short intramolecular H bond (O···O = 2.434(4) and 2.447(4) Å).

H bonding interactions between adeninium cations, adenine and hydrogen maleate are displayed in Figure 6 and Table 5.

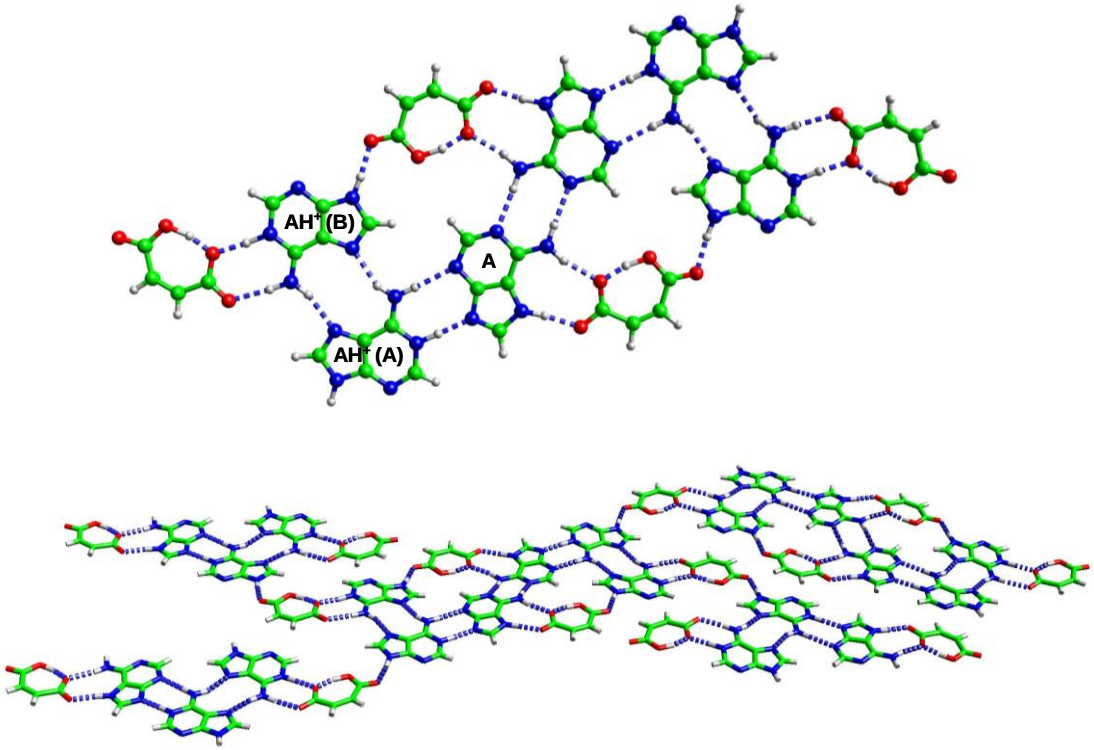

Figure 6. Hydrogen bonding motif in **3**.

The two adeninium cations, denoted adeH$^+$(**A**) and adeH$^+$(**B**), are linked by pairs of N(6)-H···N(7) hydrogen bonds generating a $R_2^2(10)$ motif. The Watson-Crick site of adeH$^+$(**A**) is used to form a double hydrogen bond with the N(3) / N(9) edge of ade. Ade utilizes its Watson-Crick site for base pairing with another ade, while N(6)-H and N(7)-H of the Hoogsteen site act as H bond donors to a carboxylate group of one of the hydrogen maleate anions giving an almost planar nine-membered ring ($R_2^2(9)$ motif). The carboxylate oxygen O(4) of the same hydrogen maleate interacts with N(9)-H of adeH$^+$(**B**). This generates $(adeH^+)_4ade_2(mal^-)_2$ entities comprising two planar $R_5^5(18)$ rings as shown in Figure 6 (top). The second hydrogen maleate anion acts as hydrogen bond acceptor to the Watson-Crick site of adeH$^+$(**B**) with O(7), O(8), N(6B)-H and N(1B)-H forming an $R_2^2(8)$ ring. In addition, this hydrogen maleate interacts with N(9)-H of adeH$^+$(**A**) through its O(5) oxygen, thus linking the $(adeH^+)_4ade_2(mal^-)_2$ units into a 2D sheet structure (Figure 6, bottom). The N(3) nitrogens of adeH$^+$(**A**) and adeH$^+$(**B**) are not

involved in H bonding. The two molecules of water of crystallization form H bonds with each other and with the hydrogen maleate oxygens O(2) and O(7) in a O(2)···O(2W)···O(1W)···O(7) pattern (see Supporting Information, Figure S8). These chains of mal^-···O(2W)···O(1W)···mal^- interactions connect the sheets of mal^-, $adeH^+$ and ade so that overall a 3D H bonded network is obtained.

Table 5. Hydrogen bonding in 3 (Å, °)

D-H···A [a]	d(D-H)	d(H···A)	d(D···A)	∠(DHA)
N(6)-H(6A)···N(1)#1	0.98(3)	2.08(3)	3.05(4)	171(2)
N(6)-H(6B)···O(1)#2	0.97(4)	1.88(4)	2.841(4)	168(3)
N(7)-H(7)···O(2)#2	1.04(4)	1.69(4)	2.720(4)	175(3)
N(6A)-H(6AA)···N(3)	0.96(4)	2.06(4)	3.018(5)	177.5(9)
N(1A)-H(1A)···N(9)	1.06(4)	1.69(4)	2.741(4)	178(1)
N(6A)- H(6AB)···N(7B)#3	0.91(4)	2.02(4)	2.868(5)	155(3)
N(9A)-H(9A)···O(5)	1.06(3)	1.68(3)	2.738(4)	174(2)
N(6B)-H(6BB)···N(7A)#4	0.95(4)	2.02(4)	2.931(4)	161(3)
N(6B)-H(6BA)···O(7)#5	1.00(4)	1.88(4)	2.872(5)	176(3)
N(1B)-H(1B)···O(8)#5	1.16(4)	1.56(4)	2.708(4)	175(3)
N(9B)—H(9B)···O(4)#3	1.00(3)	1.67(3)	2.665(4)	175(4)
O(1W)-H(1W)···O(7)#5	0.88(3)	1.90(3)	2.767(4)	170(3)
O(2W)-H(3W)···O(2)#6	0.95(5)	1.90(5)	2.829(4)	166(3)
O(2W)-H(4W)···O(1W) #3	0.83(5)	2.18(5)	2.991(5)	164(6)
O(1)-H(1C)···O(3)	1.34(4)	1.12(4)	2.434(4)	166(3)
O(6)-H(6C)···O(8)	1.14(4)	1.33(4)	2.447(4)	166(3)

[a] symmetry operation: #1: -x,2-y,-z; #2: -x,1-y,-z; #3: 1-x,1/2+y,1/2-z; #4: 1-x,-1/2+y,1/2-z; #5: -1+x,y,z; #6: 1-x,1-y,-z

4. DISCUSSION

The most notable structural features of the adeninium and benzyladeninium carboxylates described above are the presence of the non-canonical 7H-adenine tautomer in **3** and the unusual 7H,9H-tautomer of the benzyladeninium cation in **2**. Several theoretical and experimental studies have shown that the 9H-amino form is the most stable tautomer of adenine in the gas-phase and in aqueous solution.[55-57] However, while the energy difference between 9H-adenine and the minor 7H-tautomer is 7 – 8 kcal mol^{-1} in the gas-phase, the energy gap becomes significantly smaller, when electrostatic interactions with polar solvent molecules are included due to the larger dipole moment of 7H-adenine.[17,58] Consequently, both tautomers co-exist in water.[58] It is also well-documented that metal coordination to the N(9) donor site in combination with non-covalent interactions can stabilize the 7H-tautomer of adenine in the solid state.[59,60] By contrast, the presence of the minor tautomer as free molecule in the solid state (*i.e.* without metal coordination) is quite rare. Indeed, we are aware of only two examples of solid-state structures containing the 7H-tautomer of adenine; $\{[Mn(\mu\text{-}ox)(H_2O)_2](7H\text{-}ade)\cdot H_2O\}_n$[28] and $[Mg(H_2O)_6X_2\cdot 2(7H\text{-}ade)]$ ($X = Cl^-, Br^-$).[29] In the former one the minor tautomer is stabilized through a strong network of H bonds between adenine and a metal-oxalate inorganic framework. In the latter one two *cis*-coordinated water molecules form strong H bonds with the N(3),N(9) edge, thus supporting the shift of the proton from the N(9) to the N(7) position. There are five types of molecular recognition in **3**: (i) between two adeninium cations (pairs of N(6)-H···N(7) hydrogen bonds), (ii) between an adeninium cation and a neutral adenine (Watson-Crick site / N(3),N(9) edge), (iii) between two neutral adenines (pairs of N(1)-H···N(6) hydrogen bonds), (iv) between an adeninium cation and a carboxylate group (N(1)-H···O, N(6)-H···O) and (v) between an adenine and a carboxylate group (N(6)-H···O, N(7)-H···O). The latter one stabilizes the 7H-tautomer of adenine, as the proton transfer from N(9) to N(7) allows for a double hydrogen bond between the Hoogsteen site and carboxylate. The N(3),N(9) edge of the 7H-tautomer represents a double acceptor site and interacts with the protonated Watson-Crick site of an adeninium

cation. This is in contrast to the canonical 9H-tautomer where both the N(3),N(9) edge and the Hoogsteen site act as donor and acceptor sites (Scheme 1).

To the best of our knowledge, the existence of the 7H,9H-tautomer in **2** is unprecedented in solid-state structures of N^6-benzyladeninium salts. There is only one example for a crystal structure with an N^6-substituted adenine derivative protonated at N(7) and N(9), N^6-decyladeninium chloride.[61] It is worthy of note that the unusual 7H,9H and the major 3H,7H-tautomer have similar donor / acceptor dispositions: In both cases the Hoogsteen site serves as a double hydrogen bond donor site, while the N(3),N(9) edge acts as both donor and acceptor site (Scheme 1). Therefore, molecular recognition between properly arranged H bond donors and acceptors alone cannot explain the existence of the unusual tautomeric form in the crystal structure. The N(7)···O(4) distance is 2.628(2) Å suggesting a strong H bond between N(7)-H and the maleate oxygen which may partly compensate the positive charge in the imidazole ring and stabilize the rare tautomer.

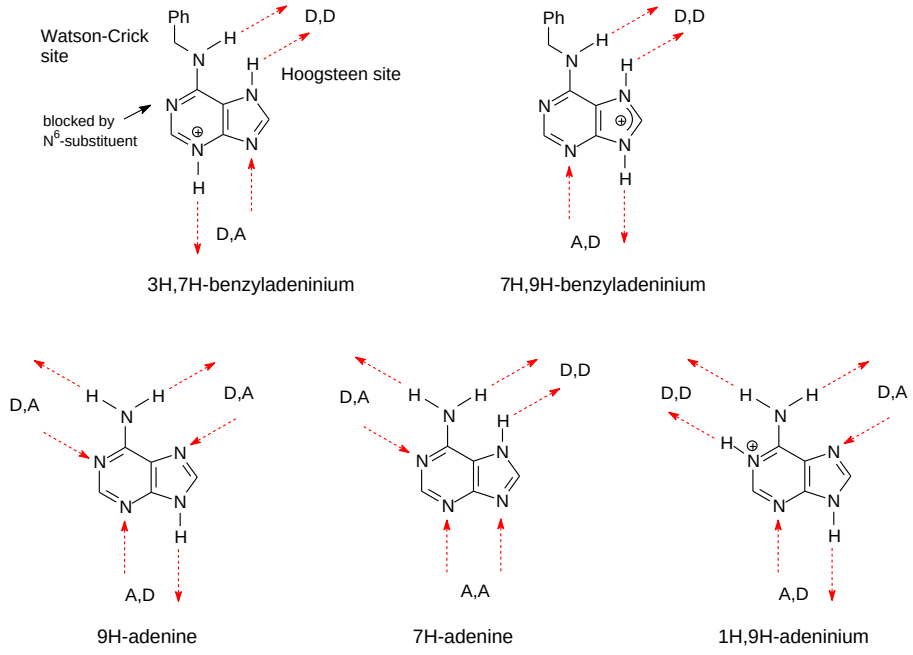

Scheme 1. Donor (D) and acceptor (A) properties of benzyladeninium, adenine and adeninium tautomers.

A building block found in all three supramolecular structures is the $R_2^2(9)$ heterosynthon based on double H bonds between a protonated Hoogsteen site and a carboxylate group. Besides the $R_2^2(9)$ heterosynthon, **1** contains an $R_2^2(8)$ homosynthon resulting from N(3)-H···N(9) interactions. N(3),N(9) double N-H···N hydrogen bonds are a common base-pairing mode which is often found in the solid state structures of adenine, adenine derivatives and corresponding salts. The other feasible $adeH^+$···$adeH^+$ self-association mode of the 3H,7H tautomer in **1** involving N(1),N(6)-H of the Watson-Crick site is precluded due to the orientation of the N^6-benzyl group. As a consequence, the typical ribbon or layer structure of cations self-associated through N(3)-H···N(9) and N(6)-H···N(1) hydrogen bonds that is frequently observed in adeninium salts is not realized in **1**. $BzadeH^+$···$bzadeH^+$ dimers similar to the $R_2^2(8)$ homosynthon in **1** are not observed in **2**, although the same self-association mode involving N(3),N(9) would be possible for the 7H,9H tautomer present in the oxalate salt. Instead, the structure is built up by $bzadeH^+$···ox^{2-}···$bzadeAH^+$ entities that are linked through single N(9)-H···ox^{2-} hydrogen bond interactions into an infinite network. In **3**, $R_2^2(8)$ and $R_2^2(10)$ homosynthons are present in addition to the $R_2^2(9)$ heterosynthon. The Watson-Crick site is not blocked and base-pairing between adenine molecules *via* N(6)-H···N(1) hydrogen bonding is observed ($R_2^2(8)$ homosynthon), while hydrogen bonding interactions between adeninium cations *via* the Hoogsteen site generate the $R_2^2(10)$ homosynthon.

Another point worthy of note is the observation of C-H···N hydrogen bonds between benzyladeninium cations in **2**. Although hydrogen-bonding interactions between aromatic C-H and heterocyclic nitrogens are well-established,[62] in nucleobase chemistry C-H···N interbase interactions are usually reinforced by strong N-H···O/N hydrogen bonds.[63-66] This is not the case here. The C(8)-H···N(3) hydrogen bond is the only interaction between neighbouring $bzadeH^+$ cations. In **2** aromatic C-H···O hydrogen bonds are present, while no C-H···N/O interactions occur in **3**.

5. CONCLUSIONS

Supramolecular structures are reproducibly and quantitatively formed by solid-state or solvent-drop grinding of mixtures of bzade and the pharmaceutically acceptable salt formers oxalic acid and maleic acid. Single-crystal X-ray analysis revealed the presence of a robust $R_2^2(9)$ heterosynthon. Strong N-H···O and charge assisted N-H^+···O^- hydrogen bonds between a carboxylate group and the Hoogsteen site of adenine and N^6-benzyladenine stabilize the unusual 7H,9H tautomer of the benzyladeninium cation in $(bzadeH^+)_2(ox^{2-})$ and the non-canonical 7H-adenine tautomer in $(adeH^+)_2(mal^-)_2 \cdot ade \cdot 2H_2O$.

ACKNOWLEDGEMENT

Financial support from Science Foundation Ireland (Stokes Lectureship to A.E. (Grant Number RSF712) and funding of the Solid State Pharmaceuticals Cluster (Grant Number RSF0812) is gratefully acknowledged.

SUPPORTING INFORMATION AVAILABLE

X-ray crystallographic data of compounds **1-3** in CIF format; additional measured and calculated XRPD patterns; view of the crystal packing of **3**. This information is available free of charge via the Internet at http://pubs.acs.org/.

REFERENCES

(1) Sadaie, M. R.; Mayner, R.; Doniger, J. *Antivir.Res.* **2004**, *61*, 1 and refs. therein.

(2) Agbottah E.; de La Fuente, C.; Nekhai, S.; Barnett, A.; Gianella-Borradori, A.; Pumfery, A.; Kashanchi, F. *J. Biol. Chem.* **2005**, *280*, 3029.

(3) Harmse, L.; van Zyl, R.; Gray, N.; Schultz, P.; Leclerc, S.; Meijer, L.; Doerig, C.; Havlik, I. *Biochem. Pharmacol*. **2001**, *62*, 341.

(4) Miller, C. O.; Skoog, F.; Von Saltza, M. H.; Strong, F. M. *J. Am. Chem. Soc*. **1955**, *77*, 1392.

(5) Dolezal, K.; Popa, I.; Krystof, V.; Spichal, L.; Fojtikova, M.; Holub, J.; Lenobel, R.; Schmülling, T.; Strnad, M. *Bioorg. Med. Chem*. **2006**, *14*, 875-884.

(6) Havlíček, L.; Hanuš, J.; Veselý, J.; Leclerc, S.; Meijer, L.; Shaw, G.; Strnad, M. *J. Med. Chem*. **1997**, *40*, 408.

(7) Veselý, J.; Havlíček, L.; Strnad, M.; Blow, J. J.; Donella-Deana, A.; Pinna, L.; Letham, D. S.; Kato, J.-Y.; Detivaud, L.; Leclerc, S.; Meijer, L. *Eur. J. Biochem*. **1994**, *224*, 771.

(8) Schang L. M.; Rosenberg A.; Schaffer P. A. *J Virol.* **2000**, *74*, 2107.

(9) Vermeulen, K.; Strnad, M.; Havlíček, L.; Van Onckelen, H.; Lenjou, M.; Nijs, G.; Van Bockstaele, D. R.; Berneman, Z. N. Exp. Hematol. **2002**, *30*, 1107.

(10) Sivakova, S.; Rowan, S. J. *Chem. Soc. Rev*. **2005**, *34*, 9.

(11) Byres, M.; Cox, P. J.; Kay, G.; Nixon, E. *CrystEngComm*. **2009**, *11*, 135.

(12) Perumalla, S. R.; Suresh, E.; Pedireddi, V. R. *Angew. Chem. Int. Ed*. **2005**, *44*, 7752.

(13) Fonseca Guerra, C.; Bickelhaupt, F. M.; Saha, S.; Wang, F. *J. Phys. Chem. A* **2006**, *110*, 4012.

(14) Laxer, A.; Major, D. T.; Gottlieb, H. E.; Fischer, B. *J. Org. Chem.* **2001**, *66*, 5463.

(15) Sečkárová, P.; Marek, R.; Malináková, K.; Kolehmainen, E.; Hocková, D.; Hocek, M.; Sklenár, V. *Tetrahedron Lett.* **2004**, *45*, 6259.

(16) Marian, C.; Nolting, D.; Weinkauf, R. *Phys. Chem. Chem. Phys.* **2005**, *7*, 3306.

(17) Huang, Y.; Kenttamaa, H. *J. Phys. Chem. A* **2004**, *108*, 4485.

(18) Kistenmacher, T. J.; Shigematsu, T. *Acta Cryst*. **1974**, *B30*, 166.

(19) Langer, V.; Huml, K. *Acta Cryst.* **1978**, *B34*, 1881.

(20) Langer, V.; Huml, K.; Zachová, J. *Acta Cryst*. **1979**, *B35*, 1148.

(21) Raghunathan, S.; Sinha, B. K.; Pattabhi, V. *Acta Cryst*., **1983**, *C39*, 1545.

(22) Soriano-Garcia, M.; Parthasarathy, R. *Acta Cryst*. **1977**, *B33*, 2674.

(23) Umadevi, B.; Stanley, N.; Muthiah, P. T.; Bocelli, G.; Cantoni, A. *Acta Cryst.* **2001**, *E57*, o881.

(24) Stanley, N.; Muthiah, P. T.; Geib, S. J. *Acta Cryst*. **2003**, *C59*, o27.

(25) Ślósarek, G.; Kozak, M.; Gierszewski, J.; Pietraszko, A. *Acta Cryst*. **2006**, *B62*, 102.

(26) However, on the basis of the geometric parameters of the purine ring a dynamic equilibrium between the 7H isomer protonated at N3 and the 9H isomer has been proposed for kinetin dihydrogenphosphate. In addition, kinetin dihydrogenphosphate was found to undergo a phase transition at 291 K with the low temperature structure containing one kinetin cation with geometric features close to those of the N3-protonated 7H tautomer and one with structural characteristics corresponding to a doubly protonated adenine with protons at N3, N7 and N9 (ref 25).

(27) García-Terán, J. P.; Castillo, O.; Luque, A.; García-Couceiro, U.; Beobide, G.; Román, P. *Inorg. Chem.* **2007**, *46*, 3593.

(28) García-Terán, J. P.; Castillo, O.; Luque, A.; García-Couceiro, U.; Beobide, G.; Román, P. *Dalton Trans*. **2006**, 902.

(29) Mastropietro, T. F.; Armentano, D.; Marino, N.; De Munno, G. *Polyhedron* **2007**, *26*, 4945.

(30) Blagden, N.; de Matas, M.; Gavan, P. T.; York, P. *Adv. Drug Deliv. Rev*. **2007**, *59*, 617.

(31) Vishweshwar, P.; McMahon, J. A.; Bis, J. A.; Zaworotko, M. J. *J. Pharm. Sci.* **2006**, *95*, 499 and refs. therein.

(32) Miroshnyk, I.; Mirza, S.; Sandler, N. *Expert Opin. Drug Deliv***. 2009**, *6*, 333.

(33) Vishweshwar, P.; McMahon, J. A.; Bis, J. A.; Zaworotko, M. J. *J. Pharm. Sci.* **2006**, *95*, 499.

(34) Trask, A. V.; Haynes, D. A.; Motherwell, W. D. S.; Jones, W. *Chem. Commun*. **2006**, 51.

(35) Trask, A. V.; Jones, W. Crystal Engineering of Organic Cocrystals by the Solid-State Grinding Approach. In Organic Solid State Reactions; Toda, F., Ed.; Springer: New York, 2005; pp 41-70.

(36) Braga, D.; Grepioni, F. *Chem. Commun*. **2005**, 3635.

(37) Caira, M. R.; Nassimbeni, L. R.; Wildervanck, A. F. *J. Chem. Soc. Perkin Trans*. *2* **1995**, 2213.

(38) Patil, A. O.; Curtin, D. Y.; Paul, I. C. *J. Am. Chem. Soc*. **1984**, *106*, 348.

(39) Pedireddi, V. R.; Jones, W.; Chorlton, A. P.; Docherty, R. *Chem. Commun.* **1996**, 987.

(40) Trask, A. V.; Motherwell, W. D. S.; Jones, W. *Chem. Commun*. **2004**, 890.

(41) Friščić, T.; Fábián, L.; Burley, J. C.; Jones, W.; Motherwell, W. D. S. *Chem. Commun*. **2006**, 5009.

(42) Shan, N.; Toda, F.; Jones, W. *Chem. Commun*. **2002**, 2372.

(43) McArdle, P.; Gilligan, K.; Cunningham, D.; Dark, R.; Mahon, M. *CrystEngComm*, **2004**, *6*, 303.

(44) CrysAlisPro, Oxford Diffraction Ltd., Version 1.171.33.31 (release 08-01-2009 CrysAlis171.NET).

(45) (a) Sheldrick, G. M. SHELXS-97, Program for crystal structure solution, University of Göttingen, Germany, 1997. (b) Sheldrick, G. M. SHELXL-97, Program for crystal structure refinement, University of Göttingen, Germany, 1997. (c) Sheldrick, G. M. SHELXTL-PLUS (VMS), Siemens Analytical X-ray Instruments, Inc., Madison, WI, 1990.

(46) Childs, S. L.; Stahly, G. P.; Park, A. *Mol. Pharmaceutics* **2007**, *4*, 323.

(47) Serjeant, E. P.; Dempsey, B. *Ionization Constants of Organic Acids in Aqueous Solution*, Pergamon, Oxford, 1979.

(48) Lide, D. R. (ed.) *CRC Handbook of Chemistry and Physics*, (84th ed.). CRC Press.

(49) Barták, P.; Bednář, P.; Stránský, Z.; Boček, P.; Vespalec, R. *J. Chromatogr. A* **2000**, *878*, 249.

(50) Taylor, R.; Kennard, O. *J. Mol. Struct*. **1982**, *78*, 1.

(51) Jin, Z. M.; Hu, M. L.; Wang, K. W.; Shen, L.; Li, M. C. *Acta Cryst.* **2003**, *E59*, o1.

(52) Darlow, S. F.; Cochran, W. *Acta Cryst*. **1961**, *14*, 1250.

(53) Fillaux, F.; Leygue, N.; Tomkinson, J.; Cousson, A.; Paulus, W. *Chem. Phys*. **1999**, *244*, 387.

(54) Raghunathan, S.; Pattabhi, V. *Acta Cryst*. **1981**, *B37*, 1670.

(55) Hanus, M.; Kabeláček, M.; Rejnek, J.; Ryjáček F.; Hobza, P. *J. Phys.Chem. B* **2004**, *108*, 2087.

(56) Lin, J.; Yu, C.; Peng, S.; Akiyama, I.; Li, K.; Lee, L. K.; LeBreton, P. R. *J. Am. Chem. Soc.* **1980**, *102*, 4627.

(57) Dreyfus, M.; Dodin, G.; Bensaude, O.; Dubois, J. E. *J. Am. Chem. Soc.*, **1975**, *97*, 2369.

(58) Gu, J.; Leszczynski, J. *J. Phys. Chem. A* **1999**, *103*, 2744.

(59) Suzuki, T.; Hirai, Y.; Monjushiro, H.; Kaizaki, S. *Inorg. Chem.* **2004**, *43*, 6435.

(60) Morel, A. C.; Choquesillo-Lazarte, D.; Alarcón-Payer, C.; González-Pérez, J. M.; Castineiras, A.; Niclós-Gutiérrez, J. *Inorg. Chem. Commun.* **2003**, *6*, 1354.

(61) Garcia-Raso, A.; Alberti, F. M.; Fiol, J. J.; Lagos, Y.; Torres, M.; Molins, E.; Mata, I.; Estarellas, C.; Frontera, A.; Quinonero, D.; Deyà, P. M. *Eur. J. Org. Chem*. **2010**, 5171.

(62) Mascal, M. *Chem. Commun*. **1998**, 302.

(63) Metzger, S.; Lippert, B. *J. Am. Chem. Soc*. **1996**, *118*, 12467.

(64) Freisinger, E.; Rother, I. B.; Lüth, M. S.; Lippert, B. *Proc. Natl. Acad. Sci*. **2003**, *100*, 3748.

(65) Amo-Ocha, P.; Sanz Miguel, P.; Castillo, O.; Sabat, M.; Lippert, B.; Zamora, F. *J. Biol. Inorg. Chem*., **2007**, *12*, 543.

(66) Tamasi, G.; Defazio, S.; Chiasserini, L.; Sega, A.; Cini, R. *Inorg. Chim. Acta* **2009**, *362*, 1011.

For Table of Contents Use Only

Supramolecular Structures and Tautomerism of Carboxylate Salts of Adenine and Pharmaceutically Relevant N^6-substituted Adenine

*Charlene McHugh and Andrea Erxleben**

Three X-ray structures of carboxylate salts of N^6-benzyladenine and adenine with different hydrogen bonding motifs are reported. Molecular recognition between the protonated purine ring and carboxylate stabilizes the unusual 7H,9H tautomer of the N^6-benzyladeninium cation and the minor 7H-adenine tautomer. Supramolecular structures are reproducibly and quantitatively formed by solid-state or solvent-drop grinding of N^6-benzyladenine and oxalic or maleic acid mixtures.